Tree Configuration Thermosyphon Study

Marcia B. H. Mantelli[*], Fernando H. Milanez[†] and Gregor Mielitz[‡]
Federal University of Santa Catarina, Florianopolis, SC, Brazil 88040-900

This work present a study on the tree configuration thermosyphon, which is composed by four parallel condensers and a single evaporator. The objective of the work is to analyze the applicability of the thermosyphon of to systems where one is interested in homogenizing the temperature inside enclosures, such as domestic and industrial ovens. A prototype of the tree configuration thermosyphon was built and tested under both natural and forced convection cooling over the condenser. The results show that for the natural convection tests, the evaporator can easily spread the vapor evenly through all the condensers, homogenizing the condensers temperatures. The same was not observed for the forced convection tests, where due to the high heat transfer coefficient not the entire condenser is necessary to dissipate the power input. As a consequence the vapor tends to concentrate in a small portion of the condenser. The measured condenser resistance was compared with models and correlations available in the literature. The results show that the overall thermal resistance of the condensers is larger than predicted by the modeling employed. However, the larger the power input, the smaller the differences between the model and experiments. The results suggest that the thermosyphon is over-dimensioned for the heat transfer levels encountered in domestic ovens. Despite the differences, the absolute value of the thermosyphon overall thermal resistance is actually very low, which demonstrates the device can be applied to isothermalize ovens and furnaces where natural convection of air is responsible for removing the heat being transferred by the thermosyphon.

Nomenclature

d	=	thermosyphon tube diameter [m]
g	=	gravity acceleration =9.81 m/s²
h	=	heat transfer coefficient [W/m²·K]
h_{lv}	=	vaporization enthalpy [J/kg]
k	=	thermal conductivity [W/m·K]
l	=	length [m]
Nu	=	Nusselt number (Eq. 7)
Nu*	=	modified Nusselt number (Eq. 5)
Pr	=	Prandtl number
q	=	total heat transfer rate in the tree configuration thermosyphon [W]
Q	=	heat transfer rate in a conventional thermosyphon [W]
r	=	thermosyphon tube radius [m]
R	=	thermal resistance [°C/W]
Re	=	Reynolds number
T	=	temperature [°C]

Greek symbols

ρ	=	density [kg/m³]
μ	=	dynamic viscosity [Pa.s]
ν	=	kinematic viscosity [m²/s]

[*]Professor, Department of Mechanical Engineering, Satellite Thermal Control Group, marcia@labsolar.ufsc.br.
[†]Research Engineer, Department of Mechanical Engineering, Satellite Thermal Control Group, milanez@labsolar.ufsc.br.
[‡]Research Assistant, Department of Mechanical Engineering, Satellite Thermal Control Group.

Subscripts

a = adiabatic zone
c = condenser, condensation
e = evaporator, external
f = condensation film
i = internal
l = liquid
t = thermosyphon, tube
v = vapor

I. Introduction

Two-phase thermosyphons are high efficiency heat transfer devices. The thermosyphon technology can be found in several heat transfer equipment, where a better temperature distribution and/or a large heat transfer capacity are desired. These equipment include heat exchangers, industrial and domestic ovens, vapor generators, etc. The LABSOLAR/NCTS Laboratory at the Federal University of Santa Catarina, in Brazil, is working on heat pipe and thermosyphon research since 1990 under funding of the Brazilian Space Agency, Petrobrás and other industries.

A typical thermosyphon consists of a metallic tube with both ends closed and filled with a certain amount of working fluid. Before filling the thermosyphon with the working fluid, the thermosyphon is evacuated so that, during operation, its internal volume is filled only with a saturated liquid-vapor mixture. The thermosyphon presents three typical regions: evaporator, adiabatic zone and condenser. Under operation, most of the liquid is in the evaporator, which is the region where the working fluid absorbs heat. The heat crosses the tube walls and reaches the liquid by conduction. The working fluid vaporizes and, due to pressure gradients, flows through the adiabatic zone, reaching the condenser. In the condenser, the vapor liquefies, releases latent heat and condenses on the internal walls of the tube. Gravity pulls the liquid film back to the evaporator, completing a thermodynamic cycle. The heat released during the vapor condensation crosses the tube walls by conduction and is rejected to the heat sink.

The thermosyphon thermal resistance is very low because during liquid-vapor phase change there is no temperature variation. The thermal resistance of the thermosyphon is basically determined by the thermal resistances of conduction through the tube walls and by the thermal resistances of vaporization and condensation of the working fluid, which are generally very small.

The tree configuration thermosyphon consists of several vertical thermosyphon condensers connected to a common evaporator in the horizontal position, as shown in Fig. 2. For applications such as bakery ovens, there are many advantages associated to this configuration instead of several parallel conventional thermosyphons. As there is only one evaporator, it is easy to transfer the heat to the working fluid by means of a single heater, which can be a gas burner or an electrical heater located underneath the evaporator. Also, the geometry of the evaporator allows for a more effective heat transfer from the oven's gas burner to the evaporator. The vapor generated in the evaporator is evenly distributed among all the condensers. The temperature levels of the several condensers are similar to each other because they all have a common vapor core in the evaporator, as will be seen later. A disadvantage of this configuration could be a more complex manufacturing.

The main objective of this work is to test the conception of the tree configuration. The main focus will be on the behavior of the parallel condensers. Experimental data from a prototype will be presented and analyzed, and the condensation process will be compared with correlations available in the literature.

II. Modeling the Thermosyphon Thermal Resistance

Given the complexity and the dependency of the physical phenomena appearing during the operation of the thermosyphon, such as boiling, condensation and vapor and liquid flows, the theoretical modeling of the thermosyphon can be very difficult. Each one of these processes presents complexities that make them difficult to predict, even when treated separately one from the other. When acting simultaneously in a confined space, the complexity increases even more. The literature presents some attempts to model the temperature and the pressure fields inside the thermosyphon using numerical methods (see Faghri[1]). The lack of flexibility and the high level of complexity of these types of models make simplified models such as the equivalent electric circuit model to be preferred. Furthermore, for application on engineering problems, one is usually interested on the global thermal resistance of the thermosyphon, and not on small details inside the thermosyphon. The thermal resistance of the thermosyphon R_t [K/W] is defined as:

$$R_t = \frac{\overline{T}_e - \overline{T}_c}{Q} \tag{1}$$

where $\overline{T}_e$ and $\overline{T}_c$ [K] are the evaporator and condenser average temperatures, respectively, and Q [W] is the thermosyphon rate of heat transfer.

Figure 1. Schematic of the tree configuration thermosyphon

In the equivalent electric circuit model, the thermosyphon total thermal resistance is computed as an association of the resistances of the individual heat transfer processes inside the thermosyphon. A model for vertical normal configuration thermosyphon in steady state conditions, which uses the analogy with electrical circuits, can be found in the literature (see Mantelli et al.[2]) is represented in Fig. 2. In the equivalent electric circuit model, the thermosyphon total thermal resistance is computed as an association of the resistances of the individual heat transfer processes inside the thermosyphon.

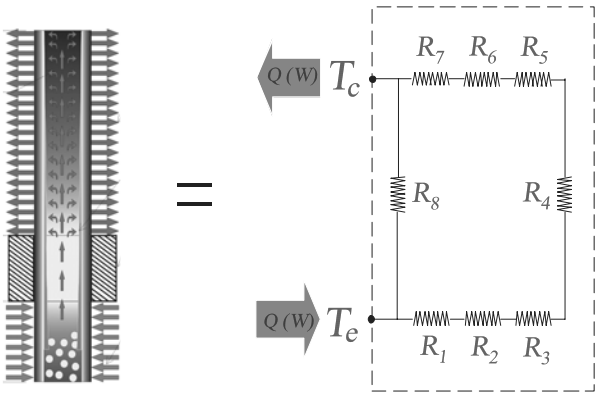

Figure 2. Thermosyphon equivalent electric circuit

Resistances R_1 and R_7 correspond to the radial conduction through the tube walls in the evaporator and in the condenser, respectively. For a circular tube, these resistances are easily calculated as:

$$R_1 = \frac{\ln(r_e / r_i)}{2\pi k_t l_e} \tag{2}$$

$$R_7 = \frac{\ln(r_e / r_i)}{2\pi k_t l_c} \tag{3}$$

The R_6 resistance is related to the process of vapor condensation in the internal walls of the condenser. It is defined as the difference between the temperature of the saturated vapor and the temperature of the internal wall of the condenser divided by the rate of heat released during the condensation of the vapor. As presented by Incropera and de Witt[3] and Bejan[4], among others, Nusselt was the first researcher to model the process of condensation on a vertical wall for the case of laminar liquid film flow and in the absence of shear stresses at the interface liquid-vapor. Faghri[1] presents a simple correlation for Nusselt's laminar condensation model, which can be written in the following form:

$$\mathrm{Nu}^* = 0.925\left(\frac{\mathrm{Re}_f}{4}\right)^{\frac{1}{3}} \tag{4}$$

where the modified Nusselt number (Nu^*) and the liquid film Reynolds number (Re_f) are defined, respectively, as:

$$\mathrm{Nu}^* \equiv \frac{h_c}{k_l}\left[\frac{v_l^2}{g}\left(\frac{\rho_l}{\rho_l - \rho_v}\right)\right]^{\frac{1}{3}} \tag{5}$$

$$\mathrm{Re}_f = \frac{4Q}{\pi d_i h_{lv} \mu_l}, \tag{6}$$

Faghri[1] also presents extensions of the Nusselt laminar condensation theory that take into account for the shear stresses resulting from the vapor flowing in the opposite direction to the liquid film. According to Faghri[1], the falling film is laminar for $\mathrm{Re}_f < 30$ and turbulent for $\mathrm{Re}_f > 2000$. For $30 < \mathrm{Re}_f < 1300$ the flow is wavy-laminar, which means laminar flow with waves on the film surface. In most the applications, the falling film flow is turbulent or wavy-laminar and the heat transfer coefficients are larger than that in the laminar regime. However, the analytical modeling of these phenomena is difficult and normally correlations obtained from experimental data are used to predict the heat transfer coefficients during condensation. Faghri[1] and Mantelli et al.[2], among others, present comparative studies between different correlations and models for the condensation heat transfer coefficients for applications in thermosyphons. Differences of up to one order of magnitude are observed between the different available correlations and models in the literature. Mantelli et al. (1999) also presented measurements of the condensation heat transfer coefficients obtained from a thermosyphon with similar characteristics to the one employed in this application. These authors show that the correlation proposed by Kaminaga et al.[5] was the one that better predicted their experimental data for the condenser. The correlation of Kaminaga et al.[5] can be written in the following form:

$$Nu \equiv \frac{h_c d_i}{k_l} = 25\,\mathrm{Re}_f^{0.25}\,\mathrm{Pr}_l^{0.4}, \tag{7}$$

The condensation resistance can be then computed as:

$$R_6 = \frac{1}{h_c\, 2\pi r_i l_c} \tag{8}$$

The R_2 resistance is related to the process of evaporation of the liquid. During the operation of the thermosyphon, the liquid pool generally does not fill the entire volume of the evaporator, or either, part of the internal wall of the evaporator is coated by the condensed film that returns from the condenser. Therefore, the thermal resistance of the evaporator is the association of two resistences in parallel: the resistance of evaporation of the condensed film and the resistance of evaporation of the liquid pool.

The process of evaporation of a liquid film in a vertical wall is similar to the process of film condensation. The results of the Nusselt condensation laminar film theory has been used (Faghri[1], Brost[6]) to predict the exchange of heat associated to the evaporation of the liquid film on the walls of the evaporator. Other correlations have been proposed for the specific process of evaporation in thermosyphons based on the Nusselt theory and that take into account also for the effect of the diameter of the pipe and the presence of nucleate boiling at the interface between the tube wall and of the liquid film, as described by Faghri[1]. The heat transfer coefficients calculated according with the Nusselt theory are generally larger than observed experimentally in thermosyphons, because the condensed film is broken and transformed into rivulets of liquid, which dries part of the evaporator wall. On the other hand, when the evaporator heat flux is high, nucleate boiling occurs in the rivulets. When the vapor bubbles inside the liquid

blow up, the rivulets are broken and liquid is spread all around the evaporator, wetting the entire internal wall and increasing the heat transfer coefficient (see Faghri[1] for more details).

The R_3 and R_5 resistances shown in the equivalent circuit of Fig. 2 appear at the liquid-vapor interface in the evaporator and in the condenser, respectively. These resistances can generally be ignored (Brost[6]). The resistance R_4 is associated with the drop of saturation temperature of the vapor due to the pressure drop of the vapor flow between the evaporator and the condenser. In general, this resistance can also be neglected.

Finally, the R_8 resistance is due to the axial heat conduction between the evaporator and the condenser through the tube walls. It can be estimated as the average length that the heat crosses between the evaporator and the condenser, which is the summation of half the length of the evaporator, half the length of the condenser and the length of the adiabatic section, divided by the thermal conductivity and by the cross-section area of the tube walls:

$$R_8 = \frac{(l_e + l_c)/2 + l_a}{k_t \pi \left(r_e^2 - r_i^2\right)} \tag{9}$$

In general, the axial conduction resistance R_8 is much larger than the other resistances of the equivalent circuit of Fig. 2, and, as it is in parallel with resistances R_1, R_2, R_3, R_4, R_5, R_6 and R_7, which are associated in series, it can be neglected. As a result, the thermosyphon total thermal resistance is given by the summation in series of the resistances R_1, R_2, R_6 and R_7. The thermophysical properties appearing in the above equations must be estimated at the average temperature of the thermosyphon, given by the arithmetic mean of the average temperatures of the evaporator and of the condenser.

The complete equivalent electric circuit for the tree configuration thermosyphon is presented in Fig. 3(a). In this figure, q [W] is the total heat input to the thermosyphon, while q_1 ,q_2 , q_3 and q_4 are the heat rejected by each one of the condensers. Similarly, $T_{c,1}$, $T_{c,2}$, $T_{c,3}$, $T_{c,4}$ are the averages of the condensers temperatures. These temperatures are, a priori, different from each other, specially when the vapor is not supplied equally among the different condensers. However, as it will be shown later in the experimental study, the condensers temperatures are practically equal to each other. In this modeling it is assumed that all the condensers are at the same temperature. Neglecting resistances R_3, R_4 and R_5, according to the discussion in the preceding paragraphs, and neglecting the thermal path by axial conduction through the tube walls, i. e., assuming R_8 much larger than the other resistances (actually it is approximately 3 to 4 orders of magnitude higher), one obtain a much simpler equivalent circuit, which is shown in Fig. 3(b). Also, the resistances associated to the condensation process inside each condenser ($R_{6,1}$, $R_{6,2}$, $R_{6,3}$, $R_{6,4}$) are assumed to be equal to each other (R_6). This assumption is made based on Eqs. (4) to (6), which show that the condensation resistance is dependent on the thermophysical properties of the working fluid, which are dependent on the temperature level and also dependent on the heat transfer rate released during the condensation process. Assuming equal temperature levels and equal heat transfer rate for all the condensers, one can assume that the condensation resistances are equal for all the condensers.

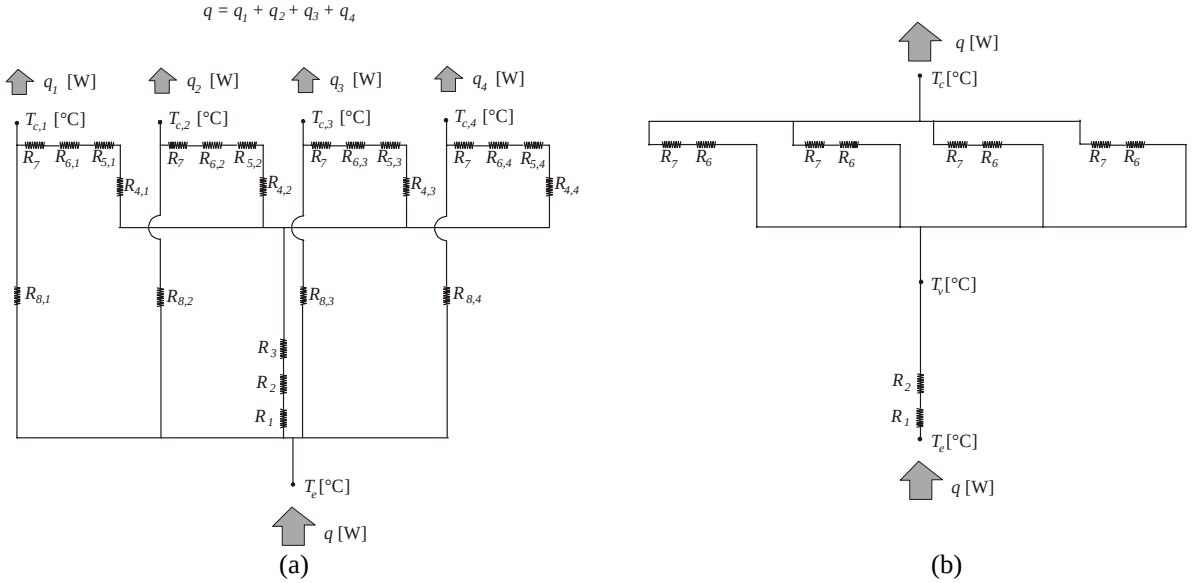

Figure 3. Tree configuration thermosyphon equivalent electric circuit: (a) complete circuit, (b) simplified circuit

Since the main objective of this work is to analyze the condensation process inside the parallel condensers and due to difficulties in assessing the evaporation resistance with the experimental set-up employed in this study (discussed later), this work will be focused on the condenser resistance only. The condenser resistance R_c is computed as:

$$R_c = \frac{T_v - T_c}{q} = \frac{R_6 + R_7}{4} \tag{10}$$

where T_v [°C] is the temperature of the vapor inside the thermosyphon.

III. Experimental Study

The tree configuration thermosyphon tested consists of four vertical condensers with a common evaporator. All tubes and caps were made of 0.2% carbon steel (AISI 1020 or C22 Standards) and connected by welding. The condensers are made of 21 mm external diameter tubes with a length of 634 mm, and the evaporator is made of a 42 mm external diameter tube with a length of 408 mm. The thickness of the tube walls are 1,5 mm and 2,65 mm for the condenser and the evaporator, respectively. These dimensions are similar to other thermosyphon configurations already tested in the laboratory (Mantelli et al.[2]). The external surface of the thermosyphon tube was electro-galvanized. The thermosyphon was evacuated to approximately 10^{-3} mbar. The selected working fluid was distilled water due to many reasons: water is cheap, easy to obtain and presents good thermal properties. The fluid was charged by means of a small tube welded in the evaporator section, as it can be observed in Fig. 2. Approximately 300 ml of distilled water was used to fill the evaporator to up to 70% of its internal volume.

Experimental Set-up

The experimental set up consists of a frame, a cooling circuit, a thermally insulated electrical heater, a power supply unit, thermocouples, a data acquisition unit and a personal computer for data storage. Figure 4(a) shows a picture of the experimental setup. A semi-cylindrical electrical resistance is attached to the bottom of the evaporator tube. Its temperature distribution as a function of its length was measured before mounting with the heater in stagnant air and it was found to be not uniform, with a maximum difference of approximately 125 K between the center and the tips of the heater. To reduce the heat losses to the surrounding environment, the evaporator tube and the assembled heater were insulated with two layers of 35mm thick glass wool. A closed water-cooling circuit is mounted around the condenser tubes to remove the heat from the thermosyphon. It has one entry and one exit tube which allow the flow of the refrigeration water from a controlled thermal bath. The setup was instrumented by means of 36 thermocouples, located according to Fig. 4 (b). After cleaning and charging, the tests described in Table 2 were conducted. The following parameters were tested: heat power levels, use of natural convection (water or air) or forced convection (circulating water) in the condenser and temperatures of the water-cooling bath.

Table 1. Parameters of the tree configuration thermosyphon tests

Test	Input power (W)	Refrigeration	Details
A	50, 100, 200, 300, 400, 500, 600, 700, 800, 900, 1000	Flowing water at 20 °C	Power level change at -every 15 min; the condenser heat is removed by forced convection
B	50, 100, 200, 300, 400, 500, 600, 700, 800	Flowing water at 40 °C	Power level change at every 15 min; the condenser heat is removed by forced convection
C	80	Stagnant air	Condenser heat removed by air natural convection; air temperature increases with time
D	500	Stagnant air	Condenser heat removed by air natural convection; air temperature increases with time
E	150	Stagnant water	Condenser heat removed by water natural convection; water temperature increases with time

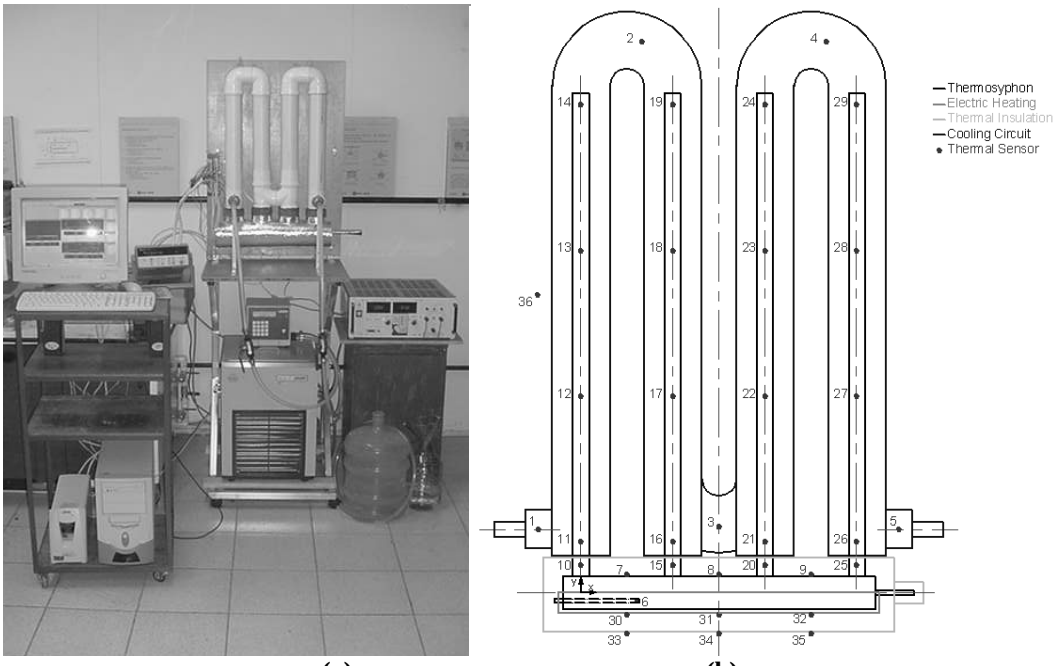

(a) **(b)**

Figure 4. Experimental setup: picture (a) and thermocouple distribution (b)

IV. Results and Discussion

The data is presented in two main groups, according to the condensers cooling type: forced convection and natural convection. The forced convection tests (Tests A and B) are analyzed first. Then, the tests that used natural convection (Tests C, D and E) are presented.

Forced convection tests

The temperature distribution for both forced convection tests (A and B) are very similar. Figure 5 shows some of the thermocouple readings of Test B as a function of time. The results and coments to be made for test B are valid for test A as well. The legend T16, T21, etc, refers to the thermocouple 16, 21, etc, according to Fig. 4 (b). The power input levels were increased every 15 minutes approximately (50, 100, 200, 300, 400, 500, 600, 700 and 800W). One can observe that, for the first two power input levels (50 and 100W, which correspond to the first 30 minutes) the temperatures did not reach steady state, as the temperature was still increasing by the time the next power level was increased. In this graph, the group of curves signaled as "Evaporator" are within a range of 5°C approximately and include T6 to T10 and T15, T20 and T25. Thermocouples T11, T16, T21 and T26 are located at the beginning of each condenser branch. Their temperature are lower than the evaporator temperatures and higher than the cooling fluid. As for the group of curves signaled "condenser + cooling fluid", it includes the remaining condenser temperatures, i.e. T12 to T14, T17 to T19, T22 to T24 and T27 to 29 plus the cooling fluid temperatures (T1 to T5). As one can see these temperatures are very close to each other.

From these results one can conclude that only a small portion of the condensers was active in Tests A and B. The vapor did not reach thermocouples T12, T17, T22 and T27 so most of the condensers length was inactive. The external convection heat transfer (water in forced convection) was so intense that only a small portion of the total available condenser length was necessary to dissipate the power input. One can also observe that T16 and T21, which correspond to the two condensers in the center of the evaporator, are approximately at the same temperature level, especially for time larger than 45 min, when the power input was larger than 300W. Thermocouples T26 and T11, which are the first and the last condensers, are at a lower level than the condensers of the center. Despite not being presented in Fig. 5, the temperatures of the electrical heater were not uniform either: T30=308°C, T31=326°C and T32=393°C for the highest power input level. That means the electrical heater provide a more intense heat flux near to T26 than near T11, which explains why T26 is larger than T11. However, T16 being larger than T26 is a surprise.

These results show that the vapor has a preferential path through the condensers located nearer the center of the evaporator. The vapor flow seems to search for the shorter way through the condenser. The forced convection tests (A and B) showed that for intense convective heat transfer external to the condensers, the system is over-dimensioned. Only a small portion of the condensers is necessary to transfer the heat power input. The remaining portion did not even start-up.

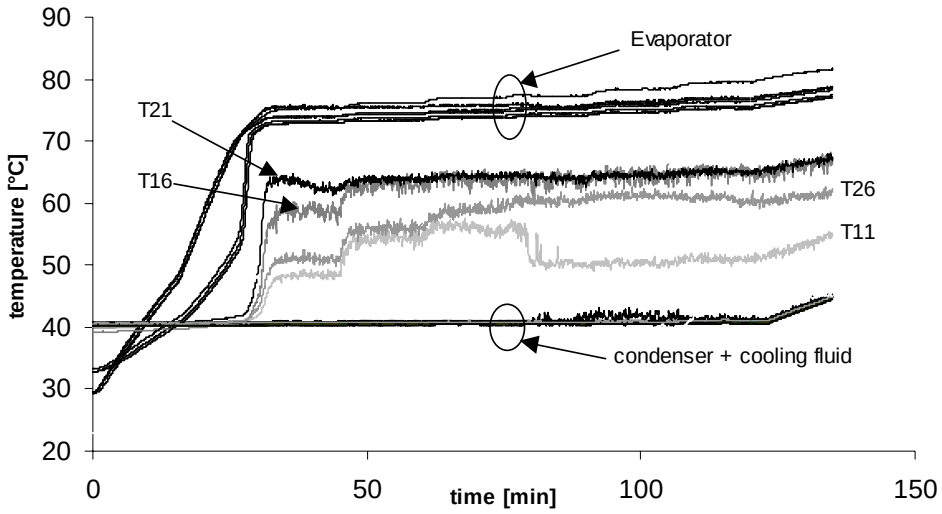

Figure 5. Temperatures as a function of time for test B

Natural Convection Tests

The effect of cooling by natural convection on the tree configuration thermosyphon was analyzed in tests C, D and E (see Table 2). Natural convection, especially with air as the cooling fluid, yields much less effective heat transfer. In test C, the heater power input was 80 W and the test lasted for a long time (almost 7 hours) in order to observe both the transient and steady state behaviors of the thermosyphon. In test D, the power input was 500 W, but the time of testing was much smaller, approximately 25 min. The thermal behavior of the thermosyphon when the heat power is turn off was also analyzed in this case. Finally, in test E, the power input was 150 W while stagnant water was confined externally to the condensers in order to obtain natural convection cooling.

The evaporator temperatures as a function of time for test C are shown in Fig. 6. The graph shows that after approximately 150 min of test the temperatures reached steady state. The four parallel condensers present very similar behavior, indicating that the vapor is distributed evenly among the four condensers in this case, contrary to the forced convection tests presented previously. There are four important groups of curves in this graph. The first group correspond to the bottom half of the condensers and the evaporator, which are within 10°C of difference among them and is located in upper region of the graph (mean temperature of 85°C). The evaporator and the bottom half of the condensers are approximately isothermal. As for the group formed by T13, T18, T23 and T28 (mean temperature of 50°), and the group formed by T14, T19, T24 and T29 (mean temperature of 38°), which are located in the upper half of the condensers, the temperature levels are lower than the bottom half of the evaporator, especially for the tip of the condensers (T14, T19, T24 and T29), which are at a temperature only slightly higher than the cooling fluid (stagnant air). As the temperature of the condensers is higher than the cooling fluid in their entire length, one conclude that the entire length of the condensers are active, i.e., are exchanging heat with the external environment. However, the upper half of the condensers are not as effective as the bottom half, i.e, the upper half of the condensers are not fully started-up yet.

The results of test D are very similar to test C, except that only T14, T19, T24 and T29 are cooler than the rest of the condenser. The power input in test D was much larger (500W) than in test C (80W) so the vapor had strength to advance further up into the condensers. Only the tips of the condensers were not fully started-up. As for test E (150W, water as cooling fluid) the results are also similar to test C: only the bottom of the condenser fully started-up, while the remaining parts are ineffective for heat transfer.

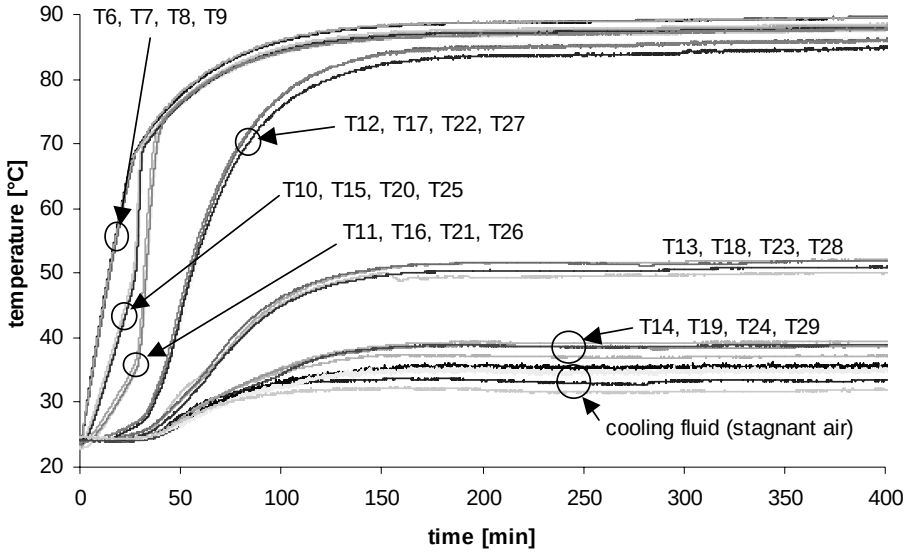

Figure 6. Temperatures as a function of time for test C

Thermal resistances

Several theoretical models and empirical correlations are available in the literature to estimate the vapor condensation resistance inside the condenser tube. Faghri[1] and Mantelli et al.[2] review some of these expressions and the results show differences of one order of magnitude in the predicted condensation heat transfer coefficient h_c appearing in Eq. (8). I this work, Re_f (defined by Eq. 6) ranges from 0.8 to 16. According to Faghri[1], the falling liquid film is laminar for $Re_f < 30$. Nusselt developed a theoretical model for laminar film flow and Faghri[1] presents a correlation for this model (Eq. 4). Kaminaga et al.[5] proposed a correlation from experimental data covering Re_f in both the laminar and the turbulent ranges (Eq. 7). Figure 7 shows a comparison between the correlation of Kaminaga et al.[5] (Eq. 7) and the correlation from Nusselt's model (Eq. 4) for a mean temperature of approximately 50°C. As one can see, Nusselt's model yields conductance values one order of magnitude larger than Kaminaga's correlation. Mantelli et al.[2] compared these two correlations along with many other correlations available in the literature against experimental data collected from a conventional two-phase thermosyphon made similarly to the condensers used in this work. Kaminaga's correlation showed the best agreeement with the experimental data. Also, Kaminaga's correlation yielded the smallest values of condensation conductance from all models tested that can be applied to laminar flow, while Nusselt's model yields the largest values of h_c. Appart from the large difference between the absolute values of the two models, they also present different behaviours with increasing power input: Nusselt's model decrease with the heat transfer rate while Kaminaga's correlation shows an increse of h_c with the heat transfer rate. In this work, Kaminaga's correlation is used in order to predict h_c due to reasons to be explained later.

Apart from the dependence on the heat transfer rate, the correlation of Kaminaga et al.[5] is also dependent on the mean temperature level. Figure 8 illustrates the dependence of the condensation resistance on both the mean temperature level and on the heat power input in the ranges of interest in this work. As one can see, the influence of the temperature is much smaller than the influence of the heat power input and can be neglected.

As already mentioned, the objective of this work is to analyze the condensation process inside the parallel condensers. The condenser resistance is defined according to Eq. (10), i.e.:

$$R_c = \frac{T_v - \overline{T_c}}{q} = \frac{R_6 + R_7}{4} \tag{11}$$

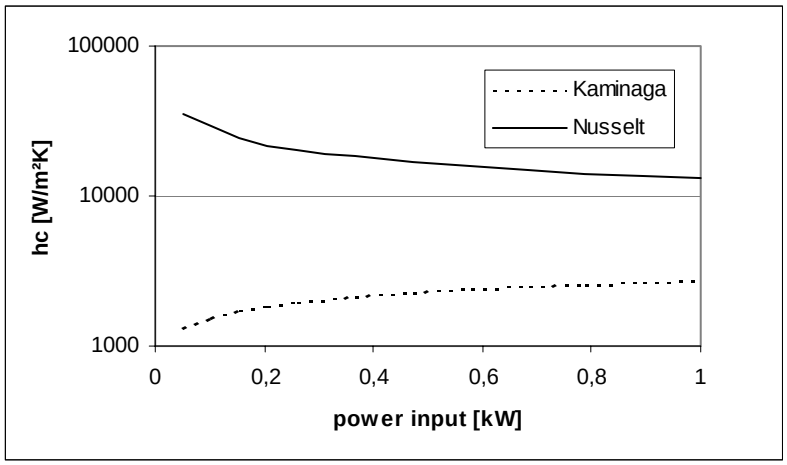

Figure 7. Comparison between the correlations of Kaminaga and Nusselt for film condensation

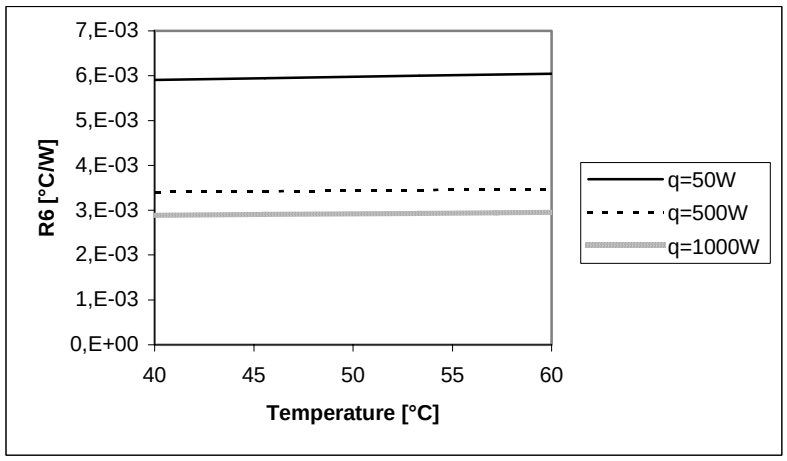

Figure 8. Effects of temperature and heat transfer rate on the condenser resistance

The vapor temperature T_v is measured using thermocouple 6, which is placed inside a needle inserted in the evaporator (see Fig. 4.b). The condenser mean temperature $\overline{T_c}$ is given by the average of the temperature readings of the active length of the condenser. For the natural convection tests (C, D, E), the entire length of the condenser is active and therefore:

$$\overline{T_c} = \left(\begin{matrix} T11+T12+T13+T14+T16+T17+T18+T19+ \\ T21+T22+T23+T24+T26+T27+T28+T29 \end{matrix} \right) / 16 \tag{12}$$

On the other hand, for the forced convection tests (A and B), only a small portion of the condensers is active. As discussed previously, T11, T16, T21 and T26 are the only thermocouples readings above the cooling fluid temperature. The other condenser thermocouples are at the same temperature as the cooling water, indicating that these portions of the condenser are inactive. Therefore, for the forced convection tests the active condenser temperature is given by:

$$\overline{T_c} = \left(T11+T16+T21+T26 \right) / 4 \tag{13}$$

Figure 9 shows a comparison between the measured and the predicted values of the condenser resistance for the forced convection tests (A and B). The experimental data was reduced using Eqs. (11) and (13), while the theoretical

prediction was obtained using Eqs. (3), (6), (7), (8) and (10). The condenser length l_c appearing in Eqs. (3) and (8) is 0.165 m, which is assumed to be approximately the active length of the condensers. This value was obtained from the observation that only thermocouples T11, T16, T21 and T26 detected the presence of vapor, as mentioned previously. As one can see, the data presents larger condenser resistances than the predictions. For small power input the differences are up to one order of magnitude, while for the highest power input tested (1000 W), the experimental value is approximately twice the predicted value of condenser resistance. As resistance R_7 is fairly well known because it is due to the radial conduction through the tube wall (Eq. 3), one can conclude that the differences between the predicted and the measured values of the condenser resistance is due to the condensation resistance R_6 (Eq. 11). As already mentioned, Kaminaga's correlation yields the smallest value of condensation resistance from the models available in the literature. Yet, the measured resistances are still larger than the predicted values. Therefore, similarly to presented by Mantelli et al.[2], Kaminaga's correlation gives the best agreement with the experimental data, despite being of up to one order of magnitude smaller than the data.

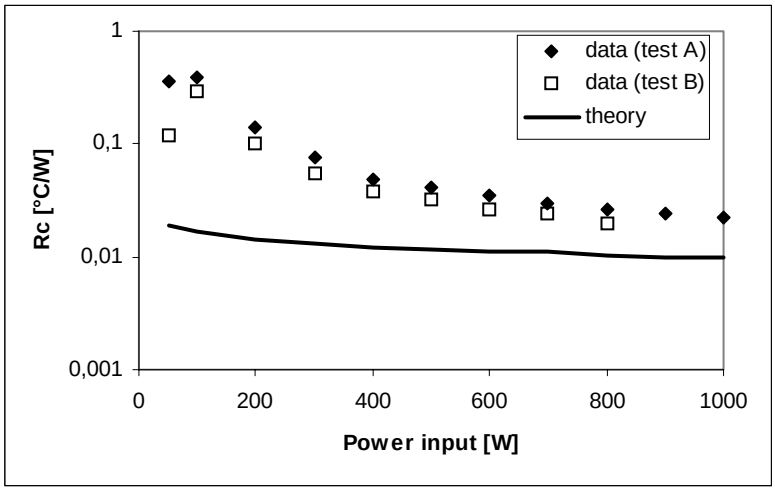

Figure 9. Theoretical and experimental values of condenser resistance for the forced convection tests

The comparison between the measured and the predicted values of the condenser resistance for the free convection tests (C, D and E) is shown in Figure 10. The experimental data was reduced using Eqs. (11) and (12), while the theoretical prediction was obtained using Eqs. (3), (6), (7), (8) and (10). The condenser length l_c appearing in Eqs. (3) and (8) is 0.594 m, which is the total length of the condensers. Similarly to the forced convection tests, the data presents larger condenser resistances than the predictions. For the smallest power input tested (test C, 80W) the difference is almost two orders of magnitude, while for the highest power input tested (test E, 500W), the experimental value is approximately one order of magnitude larger than the predicted value of condenser resistance. Again, it is expected that the differences are primarily due to the condensation resistance, which is being underpredicted by the model.

The results presented in Figures 9 and 10 would suggest that the performance of the parallel condensers is not as good as four independent regular thermosyphons were used. The modeling employed in this work showed to be adequate in predicting regular thermosyphons (Mantelli et al.[2]). Yet, for the tree configuration thermosyphon the experimental data indicate larger thermal resistances than the model. One cause for this behavior could be the size of the system, which appears to be over-dimensioned. In both Figs. 9 and 10 one can be observe that the agreement between theory and data tend to be better as the power input increases. Kaminaga's correlation predicts correctly the trend observed in the experimental data: the condenser resistance decreases with increasing heat transfer rate. For heat transfer rates larger than tested here, the results suggest that the modeling would predict the data better. For the application under consideration, which is domestic ovens, the power input is in the range of 300 to 1500W, the results show that the dimensions could be smaller and the results would be better.

Apart from the fact that the measured thermal resistance is larger than expected, the absolute value is still small. It is in the order of 10^{-2} °C/W, which means that for a power input in the order of 10^3 W the temperature drop of the condenser is approximately 10°C. Furthermore, the single evaporator showed to be very effective in distributing the

vapor equally among all the four condensers, especially when the external heat transfer coefficient is small (natural convection). This result is especially interesting when considering the fact that in the primary application of the tree configuration thermosyphon, i. e., bakery ovens, the condenser is subjected to small heat transfer coefficients (natural convection).

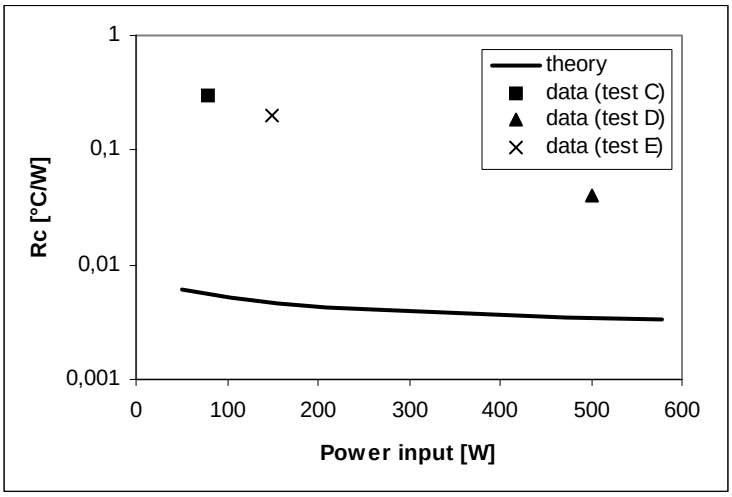

Figure 10. Theoretical and experimental values of condenser resistance for the natural convection tests

V. Summary and Conclusions

This work presents a study on the tree configuration thermosyphon, which is composed by four parallel condensers and a single evaporator. The objective of the work is to analyze the applicability of the thermosyphon of to systems where one is interested in homogenizing the temperature inside enclosures. One particular application of interest is domestic and industrial ovens. A prototype of the tree configuration thermosyphon was built and tested under both natural and forced convection cooling over the condenser. The results show that for the natural convection tests, the evaporator can easily spread the vapor evenly through all the condensers, homogenizing the condensers temperatures. This homogenization is not expected with several conventional thermosyphons in parallel. The same was not observed for the forced convection tests, where due to the high heat transfer coefficient, not the entire condenser is necessary to dissipate the power input. As a consequence the vapor tends to concentrate in a small portion of the condenser. The external conditions are important for the evaluation of the heat transfer characteristics of the thermosyphon. This means that it is impossible to obtain a thermosyphon thermal resistance, only related to the heat transfer phenomenon that happens inside the thermosyphon. Actually, the models should include the external heat transfer conditions.

The measured condenser resistance was compared with models and correlations available in the literature. The results show that the overall thermal resistance of the condensers is larger than predicted by the modeling employed. However, the larger the power input, the smaller the differences between the model and experiments. The results suggest that the thermosyphon is over-dimensioned for the heat transfer levels encountered in domestic ovens, primary objective for the development of the tree configuration thermosyphon. Despite the differences, the absolute value of the thermosyphon overall thermal resistance is actually very low, which demonstrates the device can be applied to isothermalize ovens and furnaces where natural convection of air is responsible for removing the heat being transferred by the thermosyphon.

Acknowledgments

The authors would like to acknowledge the support of CENPES-PETROBRÁS during this project.

References

[1]Faghri, A., *Heat Pipe Science and Technology*, Taylor & Francis, Bristol, 1995.

[2]Mantelli, M. B. H., Colle, S., de Carvalho, R. D. M. & de Moraes, D. U. C., "Study of closed two-phase thermosyphons for bakery oven applications," *Proceedings of the 33rd National Heat Transfer Conference*, Albuquerque, NM, 1999, pp. 1, 8.

[3]Incropera, F. P. and de Witt, D. P., *Fundamentos de Transferência de Calor e de Massa*, Ed. Guanabara Koogan, Rio de Janeiro, Brazil, 1992.

[4]Bejan, A., *Convection Heat Transfer*, John Wiley & Sons, Inc., New York, USA, 1995.

[5]Kaminaga, F., Hashimoto, H., Feroz M. D., Goto, K. and Matsumura, K., "Heat Transfer Characteristics of Evaporation and Condensation in a Two-Phase Closed Thermosyphon," *Proceedings of the 8th International Heat Pipe Conference*, Beijing, China, 1992.

[6]Brost, O., *Closed Two-Phase Thermosyphons*, Class Notes, IKE, University of Stuttgart, Germany, 1996.